

New manganese-substituted nickel hydroxides Part 1. Crystal chemistry and physical characterization

L. Guerlou-Demourgues, C. Denage, C. Delmas *

Laboratoire de Chimie du Solide du CNRS and Ecole Nationale Supérieure de Chimie et Physique de Bordeaux, Université Bordeaux I,
351 cours de la Libération, 33405 Talence Cedex, France

Received 1 August 1994; accepted 10 September 1994

Abstract

Substitution of over 20% of trivalent manganese for nickel leads to α -type nickel hydroxides. In these materials, prepared by precipitation, the compensation of the positive charge excess within the slab results from the insertion of CO_3^{2-} anions in the interslab space, as previously reported in the homologous cobalt or iron systems. These phases are unstable in the 5 M KOH electrolytic medium. The evolution of the materials during ageing has been studied by X-ray diffraction, infrared spectroscopy and magnetic measurements. It appears clearly that a structure interstratification, related to the spontaneous oxidation of the Mn^{3+} to Mn^{4+} ions, occurs. The tetravalent state of these ions in the interstratified phases leads to assume the existence of proton deficiencies within the slab since the amount of CO_3^{2-} inserted as charge compensating species is limited by steric effects.

Keywords: Nickel hydroxides; Manganese

1. Introduction

In order to stabilize the cycling between the α - and γ -hydrated nickel hydroxide varieties, the partial substitution of cobalt [1,2] and iron [3,4] for nickel in these materials has been studied in our laboratory. The α -reduced phases are stabilized by electrostatic interactions between the Fe^{3+} or Co^{3+} substituting cations within the slab and the CO_3^{2-} ions that are inserted in the interslab space in order to compensate for the positive charge excess due to the trivalent state of the substituting cations.

In the corresponding γ -oxidized phases, the study of the cationic oxidation state distribution has shown that the iron substituting ions are mainly tetravalent [5] while the cobalt ones remain at the trivalent state [6,7]. In addition, the electrochemical study has given evidence of the strong dependence between the nature of the substituting cation and the voltage of the battery using these materials as positive electrode: the presence of iron entails a voltage increase [8,9], whereas the opposite effect is observed for cobalt substitution [10,11].

In a general way, the cationic oxidation state distribution in the γ -phases must result from the ligand

field imposed by the prevailing cations and, therefore, from the size difference between the substituting cations and the nickel ones [5]. Keeping in mind that the cell voltage is directly related to the energy level of both nickel and substituting ions, cationic substitution can be a way to monitor the cell potential.

In order to improve the knowledge of these processes, the substitution of manganese has been envisaged. The characterization by X-ray diffraction and infrared spectroscopy of manganese-substituted nickel hydroxides prepared by precipitation is reported in the present paper. With a view to electrochemical cycling, the stability of these materials in concentrated KOH solution has also been studied.

2. Experimental

The materials are prepared by precipitation with 2 M NaOH from solutions of divalent manganese and nickel sulfate salts mixed in a suitable ratio. The preparation procedure, quite similar to that reported by Faure et al. [2] for the cobalt-substituted homologous materials, requires two steps:

(i) *Oxidation of the manganese ions within the solution.* The manganese sulfate solution is mixed with a con-

* Corresponding author.

centrated H_2O_2 solution (5 M). At this time, the pH of the solution stays in range from 3 to 4 and the presence of metallic cations in solution catalyses the parasitic decomposition of H_2O_2 . In fact, the oxidizing power of H_2O_2 towards the manganese ions is activated as soon as the 2 M NaOH solution is added. In order to achieve complete oxidation of the manganese ions, the H_2O_2 solution must be in large excess and the precipitation reaction must be started immediately after mixing the nickel, manganese and H_2O_2 solutions.

(ii) *Precipitation reaction.* Two precipitation procedures can be used:

(a) the 2 M NaOH solution is rapidly added to the metal-salt solution under rapid stirring until a pH value close to 10 is reached. The obtained slurry is stirred for 15 h, washed with water and acetone, and dried.

(b) another precipitation method consists in slowly dropping the metal-salt solution into the 2 M NaOH, so that the precipitation is carried out at constant pH (pH=13).

The precipitation pH has actually no influence on the formula of the obtained material but only on its crystallization state: the particle size increases with pH. This effect has previously been studied in more detail for the homologous iron system [4].

It should be noticed that some precipitation attempts have been performed without oxidizing the manganese ions with a H_2O_2 solution. In this case, the slurry colour turns gradually from green to dark brown during stirring (15 h) which suggests the gradual oxidation of the divalent manganese ions. This oxidation is immediate during the precipitation in the presence of H_2O_2 , as emphasized by the direct appearance of the brown coloured precipitate. It has been shown during the present work that, whatever the precipitation procedure, the obtained materials are similar from the structural viewpoint and exhibit identical properties. As a consequence, only the results concerning the manganese substituted hydroxides obtained by the precipitation method (b) with preoxidation of the manganese ions are reported in the following.

The preparation of composite manganese-nickel hydroxide thin films by cathodic electroprecipitation has recently been reported by Corrigan and Bendert [12]. Cordoba et al. [13] have described the chemical precipitation of similar hydroxides on conducting substrates. These authors have essentially focused their study on the role of manganese (or other metal ions) with regard to catalysis of the oxygen-evolution reaction.

3. Results and discussion

The results presented and discussed in the following deal with two material types: the materials prepared by precipitation according to the above-mentioned pro-

cedure, and those obtained after ageing of the previous ones in a concentrated KOH medium. These materials have been prepared for y manganese compositions ranging from 0.1 to 0.4; α -type phases are obtained for $y \geq 0.2$.

Related works have been carried out by Strobel and Charenton [14] concerning materials that contain exclusively manganese ions. In that case, the precipitation in oxidizing medium leads to lamellar oxides which are related to the γ -oxyhydroxides (interslab distance $d \sim 7\text{--}7.3 \text{ \AA}$). In our experimental conditions, the presence of a large amount of nickel and the oxidation conditions stabilize the divalent nickel (H_2O_2 is reducing towards Ni^{3+} ions), so that the average cationic oxidation state is lower than 3. It follows that the materials that we obtained exhibit rather the α -type structure than the γ -one. Anions and water molecules are indeed inserted between $\text{Ni}_{1-y}\text{Mn}_y(\text{OH})_2$ slabs.

3.1. X-ray diffraction study

The X-ray diffraction patterns of the materials obtained for $y=0.3$ and $y=0.1$ are given in Fig. 1 in comparison with that of the well-known unsubstituted $\beta(\text{II})$ -phase.

For the latter one, the Miller indices relative to the hexagonal unit cell have been indicated in the Figure. The interslab and metal-metal intraslab distances, which are equal to $d_{(001)}$ and $2d_{(110)}$, respectively, are close to 4.6 and 3.10 \AA , respectively.

For $y \geq 0.2$, α -type phases are obtained. Like the homologous trivalent cobalt-substituted α' -phases obtained by Faure et al. [2] and the iron-substituted phases [4], the materials crystallize in the rhombohedral system with the $P3$ structural type [15]. The structure can be depicted with a hexagonal cell, as reported in Fig. 1 for $y=0.3$. The $d_{(003)}$ and $d_{(110)}$ distances lead to the values of the interslab distance ($c_{\text{hex.}/3} = d_{(003)}$)

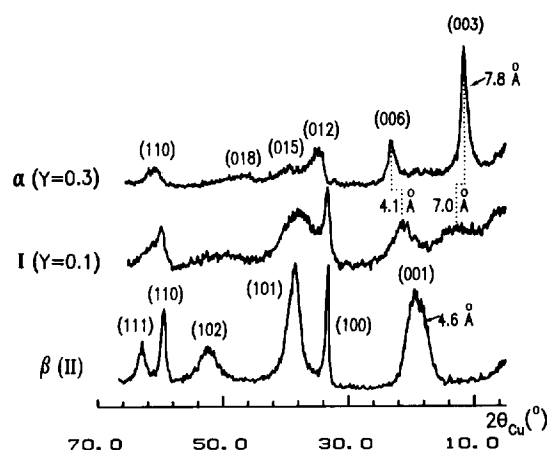


Fig. 1. Comparison of the X-ray diffraction patterns of the manganese-substituted nickel hydroxides with $y=0.3$ and $y=0.1$ composition and of the unsubstituted $\beta(\text{II})\text{-Ni}(\text{OH})_2$ phase.

and of the metal–metal intraslab distance, equal to 7.8 and 3.1 Å, respectively. As a result of the linewidth, no significant variation of the cell parameters has been detected versus the amount of manganese. The large interslab distance (~ 7.8 Å) in comparison with that of the $\beta(\text{II})$ -phase results from the intercalation of water molecules and of CO_3^{2-} ions so as to compensate the excess of positive charge due to Mn^{3+} ions within the slab. This behaviour, already observed in the homologous cobalt and iron systems [2,4], is fully confirmed by the infrared study presented in Section 3.2.

For $y=0.1$, the X-ray diffraction pattern (Fig. 1) displays similarities with that of the $\beta(\text{II})$ -phase in the $30^\circ \leq 2\theta \leq 70^\circ$ range. Below 30° , two lines broader than those present on the X-ray pattern of the α -phase are observed. The reticular distances corresponding to these two lines are not submultiple of one another, so that no indexation is possible. This behaviour suggests a disorder in the periodicity of the (00 l) planes. Indeed, for $y < 0.2$, as previously observed in the cobalt system [6], the CO_3^{2-} amount required to perform the charge compensation is not sufficient to lead to a homogeneous distribution of these ions within the interslab space, so that a segregation occurs. This leads to an interstratified structure (designated by I) that can be considered as a packing of α - and $\beta(\text{II})$ -motives randomly distributed along the c axis, as schematized in Fig. 2.

Taking into consideration the respective interslab distances of both α - and $\beta(\text{II})$ -motives, equal to 7.8 and 4.6 Å, respectively, it is possible, by a theoretical calculation performed from the method of Hendricks and Teller [16,17], to simulate the variation of the diffracted intensity versus the diffraction angle for various values of the concentration ratio

$$r_\beta = \frac{\beta(\text{II})}{\alpha + \beta(\text{II})}$$

As reported in a previous paper dealing with interstratification in cobalt and iron layered double hydroxides [15], for both extreme r_β values, the simulated 'patterns' are quite similar to those of the well-crys-

tallized $\beta(\text{II})$ - and α -materials, respectively. In a given structure, when the amount of the type of interslab space initially present decreases in favour of the other type, a broadening and a shift of the diffraction lines simultaneously occur. For intermediate compositions, the lines seem to vanish as a result of the very disordered character of the structure.

Comparison of the simulated spectra to the experimental X-ray diffraction pattern allows the r_β value characteristic of a given material to be evaluated. Fig. 3 shows that the positions and shapes of the two lines in the experimental spectrum of the $I(y=0.1)$ phase (5 – 30° angular range) are in good agreement with the evolution of diffracted intensity calculated for $r_\beta=0.55$.

3.2. Infrared spectroscopy study

Measurements were performed with a Perkin-Elmer 983 spectrometer on powders dispersed in hexachlorobutadiene in the 1000 – 4000 cm^{-1} range. The infrared (IR) spectra of the manganese-substituted nickel hydroxides are given in Fig. 4 for $y=0.1$ and $y=0.3$ in comparison with the spectrum of the unsubstituted $\beta(\text{II})$ -phase.

As the IR spectra of the $\beta(\text{II})$ - and α -type phases have been intensively commented elsewhere in the case

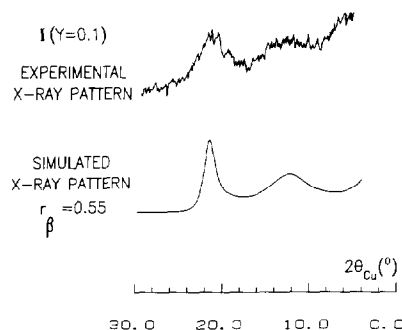


Fig. 3. Comparison of the experimental X-ray diffraction pattern of the interstratified I ($y=0.1$) phase (5 – 30° angular range) with that simulated according to the method of Hendricks and Teller for $r_\beta=0.55$.

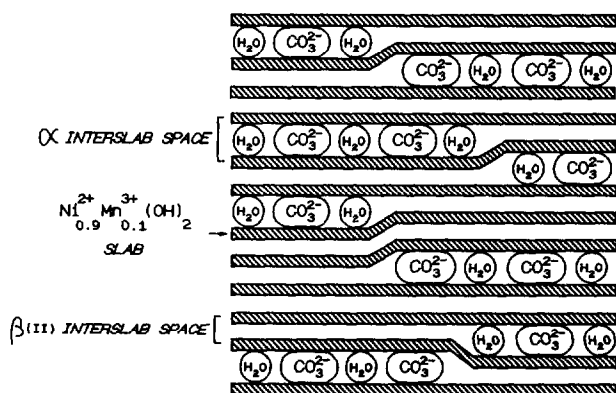


Fig. 2. Schematic representation of the interstratified structure.

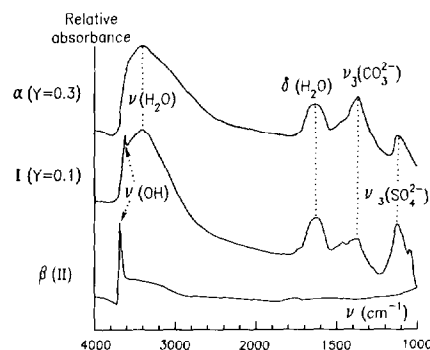


Fig. 4. Comparison of the infrared spectra of the manganese-substituted nickel hydroxides with $y=0.3$ and $y=0.1$ composition and of the unsubstituted $\beta(\text{II})$ - $\text{Ni}(\text{OH})_2$ phase.

of the homologous cobalt- and iron-substituted materials [18,4], the discussion is focused here on the interstratified phase.

The IR spectrum of this phase is intermediate between those of the α -phase and of the $\beta(\text{II})$ -phase.

(i) The narrow band at 3650 cm^{-1} which is assigned to the $\nu(\text{OH})$ stretching vibration of OH groups is characteristic of $\beta(\text{II})$ -type motives. Let us recall that, in the case of the α -phase (Fig. 4), the hydrogen bonding between the slab OH groups and the interlamellar water molecules leads to a broadening of the $\nu(\text{OH})$ band which is therefore superimposed on the $\nu(\text{H}_2\text{O})$ band (around 3400 cm^{-1}). The $\delta(\text{H}_2\text{O})$ vibration mode gives rise to a band at 1650 cm^{-1} .

(ii) The bands at 1360 and 1150 cm^{-1} are respectively due to the CO_3^{2-} ions (in D_{3h} symmetry) inserted in the interslab space of the α -motives and to the SO_4^{2-} ions (in T_d symmetry) mainly adsorbed on the grain surface, as reported in more detail in the case of the iron system [4]. Indeed, in the α -phases, the interslab distance is around 7.8 \AA whereas the presence of SO_4^{2-} ions between the $\text{Ni}_{1-y}\text{Mn}_y(\text{OH})_2$ slabs would require an interslab distance close to 9 \AA , as shown by Faure et al. [2] for the homologous cobalt system.

It is therefore clear that the simultaneous presence of both α - and $\beta(\text{II})$ -motives and, therefore, the interstratified structure of the material with $y=0.1$ composition is fully confirmed by the IR study.

3.3. Structural evolution of the precipitated phases in concentrated KOH medium

3.3.1. X-ray diffraction study

The stability in 5 M KOH medium of the manganese-substituted nickel hydroxides ($0.1 \leq y \leq 0.4$) has been tested for several durations. The modification of the X-ray diffraction patterns during ageing is shown in Fig. 5 for the $y=0.3$ substitution amount. The 'a' and 'A' indices correspond to the materials recovered after a one-day and a one-month long test, respectively.

Though the X-ray diffraction spectrum after a one-day test is almost not modified, strong structural mod-

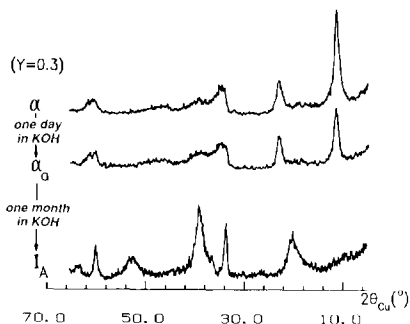


Fig. 5. Evolution of the X-ray diffraction patterns during a stay of an α -($y=0.3$)nickel hydroxide in 5 M KOH medium.

ifications occur after a one-month stay in KOH solution. Indeed, the change of the (003) and (006) lines (Fig. 5) into one broad asymmetric line ($d \sim 4.3\text{ \AA}$) shows that a structure interstratification has occurred. Comparison of the position and shape of this line to the previously reported theoretical evolution suggests that the structure of the obtained interstratified material is built up of a large amount of β -type motives ($r_{\beta/\alpha+\beta} \sim 0.70$). It should be noticed that the interstratified material resulting from ageing has been designated by I_A in order to prevent it from being confused with the interstratified phase freshly obtained by precipitation for $y=0.1$ (designated by I). This distinction is based on the difference between the interstratification processes that occur for the two materials, as it will also be discussed in the companion paper, Part 2, see Ref. [19].

Similar modifications of the material are observed during ageing for the $y=0.2$ and $y=0.3$ compositions. Simulation of the X-ray diffraction patterns by the method of Hendricks and Teller shows that amount of β -type interslab spaces (r_β) is close to 0.75 for both materials.

As far as the $y=0.4$ composition is concerned, a two-phase mixture constituted of a γ -oxyhydroxide and of an I_A -type phase appears after a one-month long test in KOH of the freshly precipitated phase. This behaviour will be discussed in the companion paper, Part 2, see Ref. [19].

3.3.2. Infrared study

The evolution of the spectra during ageing in KOH of an α -precipitated phase is shown in Fig. 6 for $y=0.3$. The similarity of the spectra of the starting α -phase

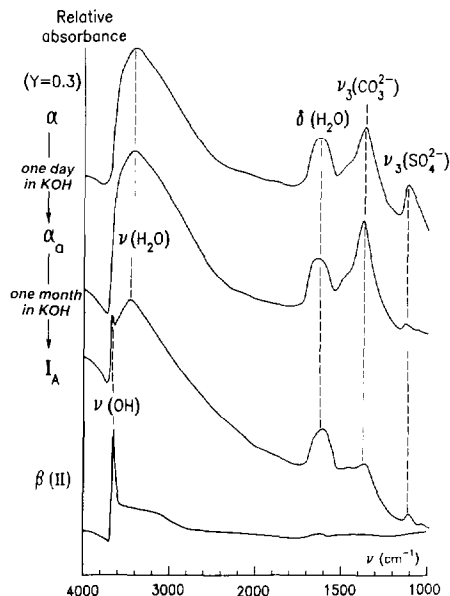


Fig. 6. Evolution of the infrared spectra during a stay of an α -($y=0.3$)nickel hydroxide in 5 M KOH medium.

Table 1
Evolution of the average cationic oxidation states with y during ageing of the manganese-substituted materials in 5 M KOH medium

y	Freshly precipitated materials		After one-day test in KOH		After one-month test in KOH	
	Phase type	Oxidation state	Phase type	Oxidation state	Phase type	Oxidation state
0.1	I	2.13	I_a	2.14	I_A	2.16
0.2	α	2.33	I_a	2.38	I_A	2.42
0.3	α	2.36	α_a	2.50	I_A	2.62
0.4	α	2.46	α_a	2.60	Phase mixture	2.77

Table 2
Evolution of the experimental and calculated Curie constants as well as of the θ_p paramagnetic Curie temperatures for the manganese-substituted nickel hydroxides ($0.0 \leq y \leq 0.4$)

y	Phase	Slab formula	Curie constants		θ_p (K)
			Calculated	Experimental	
0	α	$Ni_{1.00}^{2+}$	1.00	1.18	10
0.1	I	$Ni_{0.91}^{2+}Mn_{0.05}^{3+}Mn_{0.04}^{4+}$	1.13	1.41	14
	I_A	$Ni_{0.91}^{2+}Mn_{0.02}^{3+}Mn_{0.07}^{4+}$	1.10	1.28	15
0.2	α	$Ni_{0.80}^{2+}Mn_{0.07}^{3+}Mn_{0.13}^{4+}$	1.25	1.47	15
	I_A	$Ni_{0.80}^{2+}Mn_{0.20}^{4+}$	1.17	1.30	8
0.3	α	$Ni_{0.70}^{2+}Mn_{0.24}^{3+}Mn_{0.06}^{4+}$	1.53	1.66	21
	I_A	$Ni_{0.70}^{2+}Mn_{0.30}^{4+}$	1.26	1.19	21
0.4	α	$Ni_{0.60}^{2+}Mn_{0.34}^{3+}Mn_{0.06}^{4+}$	1.13	1.69	4

and of the α_a one-day aged material is consistent with the X-ray diffraction study which has shown that the one-day aged material still exhibits an α -type structure, as emphasized in Fig. 5. The decrease in intensity of the $\nu_3(\text{SO}_4^{2-})$ band and conversely the slight increase of the $\nu_3(\text{CO}_3^{2-})$ band can be attributed to a spontaneous exchange of SO_4^{2-} ions, mainly adsorbed on the grain surface, for CO_3^{2-} ions, as previously reported in the case of the cobalt- or iron-substituted homologous materials [4,2].

After one month in KOH medium, the sharp $\nu(\text{OH})$ band characteristic of 'free' OH groups and therefore of $\beta(\text{II})$ -type motives appears at 3650 cm^{-1} , while the intensity of the $\nu_3(\text{CO}_3^{2-})$ band at 1360 cm^{-1} due to the species inserted in the α -type interslab spaces strongly decreases. These evolutions suggest the appearance of some β -type interslab spaces at the expense of α -ones, which is in full agreement with the structure interstratification shown by the X-ray diffraction pattern in Fig. 5.

3.3.3. Evolution of the cationic oxidation state

The average oxidation state of the cations (nickel and manganese) has been determined by iodometry titration. The values obtained for the freshly precipitated phases and for the materials resulting from their ageing

in KOH solution (one-day and one-month long tests) are summarized in Table 1.

The overall results show that the cationic oxidation states are close to $(2+y)$ in the freshly precipitated materials and to $(2+2y)$ in the one-month aged materials with intermediate values for the one-day aged materials. These results suggest that the manganese ions may be mainly at the trivalent state in the starting phases ($(1-y)\text{Ni}^{2+}$ and $y\text{Mn}^{3+}$) as previously observed for the homologous cobalt and iron systems [2,4], while the final interstratified materials may contain mainly tetravalent manganese ions ($(1-y)\text{Ni}^{2+}$ and $y\text{Mn}^{4+}$). The

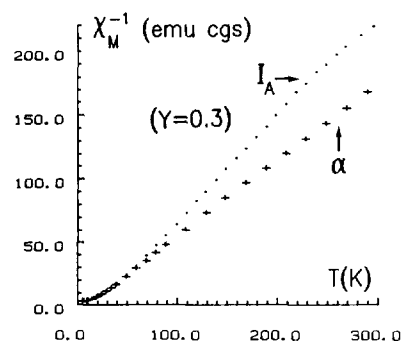
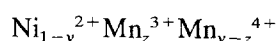


Fig. 7. Thermal variation of the reciprocal molar magnetic susceptibility of the manganese-substituted α - and I_A -materials with $y=0.3$.

reducing character of Mn^{3+} ions in this structure leads to a spontaneous partial oxidation of the material which entails an overall cationic oxidation state always larger than $(2+y)$ in the freshly precipitated materials.

This evolution is corroborated by the study of the magnetic properties. The magnetic susceptibilities of the α - and I_A -phases have been measured with a DSM8 susceptometer (MANICS) over the 4–300 K temperature range. As the aged material with $y=0.4$ composition is constituted of a two-phase mixture, its magnetic behaviour has not been discussed. The thermal variations of reciprocal magnetic susceptibility, reported in Fig. 7 for the α - and I_A -materials with $y=0.3$, give evidence of a Curie–Weiss-type behaviour. The small positive values of the paramagnetic Curie temperatures are characteristic of predominant ferromagnetic interactions within the slabs. The experimental Curie constants determined for the overall composition series are summarized in Table 2, as well as the theoretical Curie constants calculated, according to the spin only model, for the following cationic distribution (all the cations being in the high spin configuration):



where z is deduced from the average cationic oxidation state of the materials, reported in Table 1.

The general trends of the calculated and experimental Curie constant values are in good agreement and confirm that the manganese ions are mainly trivalent with the high spin configuration in the freshly precipitated materials and are oxidized to the tetravalent state in the I_A -aged materials. In addition, no tridimensional order has been detected as a result of the large interslab spaces.

4. Conclusions

In cobalt- or iron-substituted nickel hydroxides, interstratification is observed when the amount of trivalent cation is not sufficient to allow the anions inserted as charge compensating species to occupy all of the interslab spaces (i.e., for $y \leq 0.1$) [3,6]. A similar behaviour occurs for manganese-related phases.

In addition, spontaneous oxidation of Mn^{3+} to Mn^{4+} ions during ageing of the manganese-substituted nickel hydroxides entails also an interstratification phenomenon for $y \geq 0.2$. Actually, in this case, the charge compensation cannot be exclusively performed by anionic insertion as a result of steric reasons. The existence of proton deficiencies within the slab may therefore be assumed to perform the overall charge balance.

References

- [1] C. Delmas, J.J. Braconnier, Y. Borthomieu and P. Hagenmuller, *Mater. Res. Bull.*, **22** (1987) 741.
- [2] C. Faure, C. Delmas and P. Willmann, *J. Power Sources*, **35** (1991) 249.
- [3] L. Demourgues-Guerlou, J.J. Braconnier and C. Delmas, *J. Solid State Chem.*, **104** (1993) 359.
- [4] L. Demourgues-Guerlou and C. Delmas, *J. Power Sources*, **45** (1993) 281.
- [5] L. Demourgues-Guerlou and C. Delmas, *J. Solid State Chem.*, in press.
- [6] Y. Borthomieu, *Thesis*, University Bordeaux I, 1990.
- [7] C. Faure, *Thesis*, University Bordeaux I, 1990.
- [8] L. Demourgues-Guerlou and C. Delmas, *J. Electrochem. Soc.*, **141** (1994) 713.
- [9] O. Glemser, J. Bauer, D. Duss, J. Harms and H. Low, *Proc. 16th Int. Power Sources Symp.*, 1988.
- [10] C. Faure, C. Delmas and P. Willmann, *J. Power Sources*, **36** (1991) 497.
- [11] R.D. Armstrong, C.W.D. Briggs and E.A. Charles, *J. Appl. Electrochem.*, **18** (1988) 215.
- [12] D.A. Corrigan and R.M. Bendert, *J. Electrochem. Soc.*, **136** (1989) 723.
- [13] S.I. Cordoba, R.E. Carbonio, M. Lopez Teijelo and V.A. Macagno, *Electrochim. Acta*, **31** (1986) 321.
- [14] P. Strobel and J.C. Charenton, *Rev. Chim. Miner.*, **23** (1986) 125.
- [15] C. Delmas, C. Fouassier and P. Hagenmuller, *Physica*, **99b** (1980) 81.
- [16] S.B. Hendricks and E. Teller, *J. Chem. Phys.*, **10** (1942) 147.
- [17] Y. Borthomieu, L. Demourgues-Guerlou and C. Delmas, in J. Rouxel, M. Tournoux and R. Brec (eds.), *Proc. Int. Symp. Soft Chemistry Route to New materials, Nantes, France, Sept. 6–10, 1993*.
- [18] C. Faure, Y. Borthomieu, C. Delmas and M. Fouassier, *J. Power Sources*, **36** (1991) 113.
- [19] L. Guerlou-Demourgues and C. Delmas, *J. Power Sources*, **52** (1994) 283–288.